



Evaluation of Naturally Occurring Radionuclides Concentration and Associated Radiological Health Risks in Agricultural Soils from Iwerele, Oyo State, Nigeria.

Aluko, T. J.¹, Olagbaju P. O.² and Ikuemonisan, F.E.³

¹ Department of Physical Sciences Chrisland University, Abeokuta Ogun State Nigeria

²Department of Physics, North-West University South-Africa.

³Department of Physical Science Education Lagos State University of Education Lagos State Nigeria.

*Corresponding Author: alukotywo@gmail.com; +2348030477684

Abstract

Artisanal and small-scale mining activities often pose environmental and health risks to surrounding ecosystems. This study evaluates radiological hazards and potential exposure levels in soils from active and abandoned mining sites in Iwere-Ile, Oyo State, Nigeria. Twenty-two soil samples were analyzed using a Gamma-ray Spectrometer with a NaI(Tl) detector to determine the activity concentrations of naturally occurring radionuclides. The mean specific activities of ⁴⁰K and ²³²Th contributed about 15% and 9%, respectively, to the total radioactivity. The absorbed dose rate from terrestrial gamma radiation ranged from 5.86 to 217.48 nGy h⁻¹, averaging 58.06 nGy h⁻¹, slightly above the UNSCEAR global reference value of 55 nGy h⁻¹. The annual effective dose equivalent (AEDE) varied between 0.02 and 0.76 mSv yr⁻¹, remaining below the 1 mSv yr⁻¹ public dose limit. Although the annual gonadal dose equivalent (AGDE) exceeded international recommendations, the internal and external hazard indices were both less than unity, indicating minimal radiological threat. Overall, agricultural activities in the area can be considered radiologically safe despite ongoing mining operations.

Keywords: Natural radioactivity, Radiological hazard assessment, Gamma-ray spectrometry
Mining environment, Soil contamination

Received: 8th Sept, 2025 Accepted: 29th Nov, 2025 Published Online: 25th Dec, 2025

Introduction

The economy of Nigeria significantly relies on revenues generated from mineral resources. Given the fluctuations in global market prices and the unpredictable state of the worldwide economy, there is an increasing necessity to optimize the extraction of solid minerals and agricultural outputs, among other resources. The mining practices employed by small-scale operators can have detrimental effects on the environment, particularly concerning soil, water, and agricultural products cultivated near mining locations. Chemical elements having unstable isotopes that release ionizing radiation during decay are known as

radionuclides. With limited lives that range from a few fractions of a second to hundreds of years, these isotopes are referred to as radioactive isotopes. Three types of radiation are released throughout the degradation process, they are alpha particles (α), beta particles (β), and gamma rays (γ) (Orosun et al., 2022). Further releases of radionuclides into the environment come from industrial operations such mining, milling, and fertilizer manufacture (IAEA, 2014). Analysis of radionuclides in samples involves the quantitative examination of energy spectra in the gamma-ray sources and is commonly used in astrophysical, nuclear, and geological

research facilities. Gamma rays, which are characterized by their elevated photon energy and frequency, represent the most powerful form of electromagnetic radiation. Their significant penetrating ability makes them physically comparable to all other forms of radiation.

Radiation absorption rates vary by country and region. Several factors, such as the extent of mining and processing of radioactive materials, altitude relative to sea level, local geological conditions, and waste disposal practices at mines, impact this variation. Diverse methodologies have been employed around the world to gauge natural background radiation levels. These approaches have included the use of ionization chambers and portable or aerial scintillation counters. Additionally, laboratory analyses of radioactive substances present in soil and rock samples have been used to estimate average radiation exposure across various countries. Previous studies and initiatives have focused on assessing radiation exposure and radionuclide spread in mining sites worldwide. Research carried out by Beretka and Mathew (1985) and Kurnaz et al (2007) emphasized the significant part played by natural radionuclides like ^{226}Ra , ^{232}Th , and ^{40}K in causing occupational radiation exposure among miners, stressing the importance of consistent monitoring of their impacts on workers. Furthermore, Jibiri, and Okeyode, (2012) reported that radiation dose levels in soils from Southwestern Nigeria surpassed the global average, highlighting the significance of localized radiological assessments in mining areas. Extensive research efforts by Tufail et al (2006) have contributed substantially to understanding public exposure to ionizing radiation and to developing strategies for minimizing radiological risks across different environments. Based on evaluations using radiation hazard indices, these studies concluded that the measured natural radioactivity in the investigated regions remains within safe limits and poses no significant health concern. Similarly, assessments performed at a mining site in Osun State and within the International Institute of Tropical Agriculture (IITA) recorded

comparatively low radionuclide activities, as identified through advanced gamma-ray spectrometric analyses (Arogunjo *et al.* 2004, Ajayi and Ibikunle, 2013). The current investigation focuses on quantifying radiation exposure originating from naturally occurring radionuclides in soil samples obtained from mining pits and on characterizing the associated radiological hazard parameters. This research is motivated by the growing need to promote sustainable mining practices that limit environmental contamination and public health risks, particularly in economically mining-dependent communities.

Materials and Methods

Location and geology of the Study Area

This research investigates three Local Government areas within Oyo State: Iwajowa, Ibarapa North, and Ibarapa South, all located in the Oke-Ogun region. The state covers roughly 10 km², and is geographically delimited by latitude 7°30' N to 8°00' N and longitude 3°02'24" E to 3°02'28" E. A key hydrological feature of the region is the River Oyan, which flows north to south, acting as the main drainage system and effectively dividing the area into two separate halves. Geologically, the study area lies within a zone shaped by Late Precambrian to Early Proterozoic orogenic activities, situated to the east of the West African Craton (Oyawoye, 1964; Rahaman, 1976). It forms part of the Nigerian Basement Complex, which extends westward and merges with the Dahomeyan formations of the Dahomey–Togo–Ghana belt (Turner *et al.*, 1983; Rahaman, 1988). The basement rocks are bounded on the eastern and southern sides by sedimentary deposits ranging from the Mesozoic to recent periods (Obaje, 2009). Rocks of the Basement Complex show a complex geological history involving intense thermal and tectonic events that produced crustal folding, compression, and orogeny, followed by prolonged erosion that resulted in the present gentle topography (Ajibade & Wright, 1989). Based on structural, lithological, tectono-stratigraphic, and geochronological studies, the Southwestern Nigerian Basement Complex evolved through four major orogenic events (Rahaman, 1988). The area rests upon some of the most ancient

rock formations, where muscovite granite gneiss predates accompanying sericite phyllites and quartzite units.

Soil Sample Collection Procedure

A total of twenty-two soil samples were systematically collected from both active and abandoned mining pits using a soil auger at

depths between 0 and 30 cm. The precise geographic coordinates of each sampling site were recorded with a Global Positioning System (GPS). To preserve the integrity of the samples during transport, each was properly labeled, sealed in a tagged nylon bag, and transported to the Radiation Laboratory of the Federal University of Agriculture, Abeokuta, Nigeria, for subsequent radionuclide analysis.

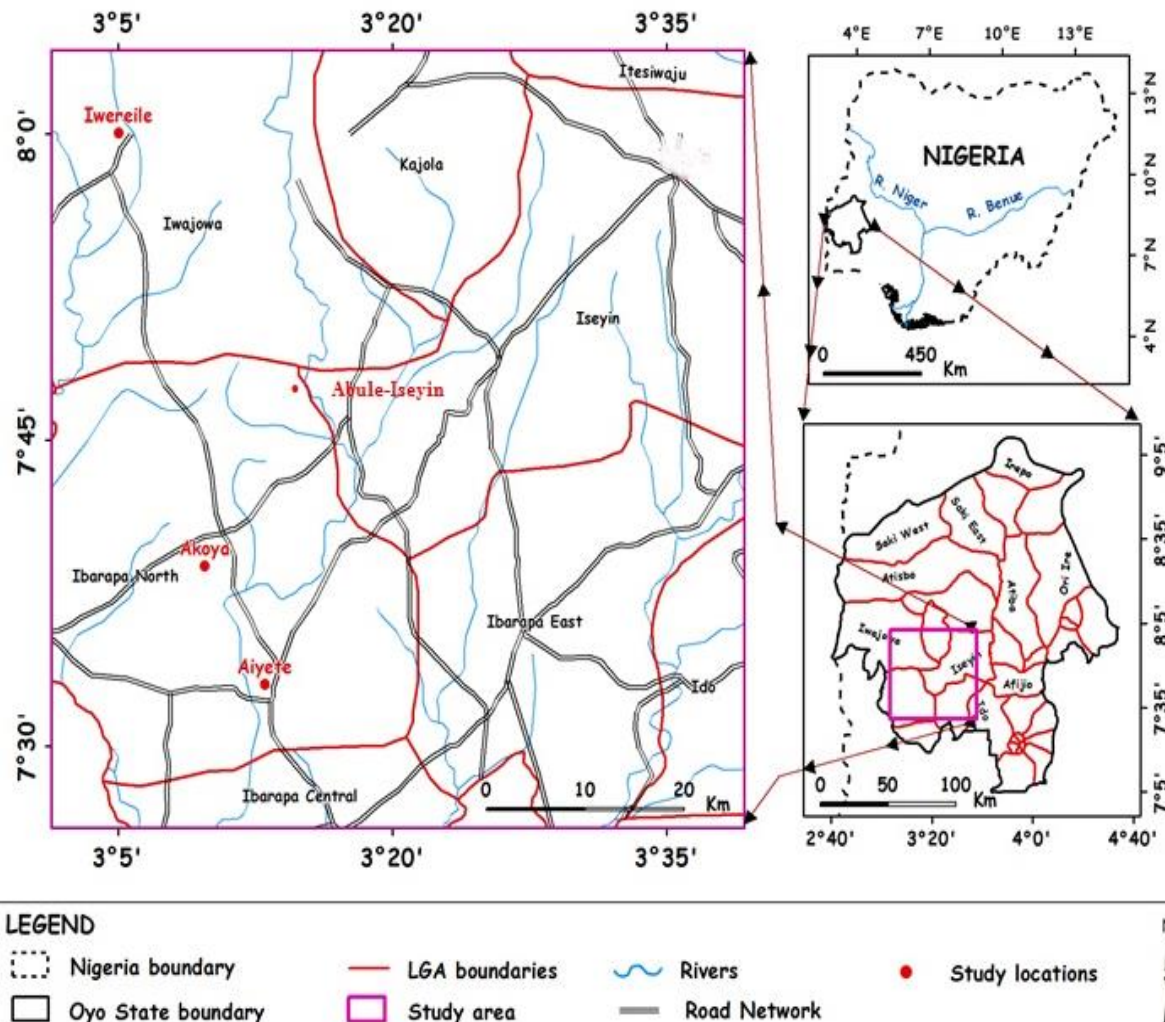


Figure 1: Location Map of the Study Area

Sample Preparation

The soil samples collected were prepared by first air-drying them to remove residual moisture. Once dried, each sample was finely ground using a mortar and pestle to enhance its surface area for analysis. The resulting powder was homogenized by sieving through a 2 mm

mesh. An exact mass of 250 g from each homogenized sample was then weighed, properly labeled, and placed into clean white plastic containers with the same geometry as those used for gamma spectrometer calibration. To prevent the escape of gaseous radionuclides such as radon isotopes (^{220}Rn and ^{222}Rn), the containers were securely sealed. The sealed

Evaluation of Naturally Occurring Radionuclides Concentration and

samples were left undisturbed for a minimum of 30 days to allow secular equilibrium to be established—this being the condition in which the activity concentrations of the decay products become equivalent to those of their parent radionuclides. Radionuclides achieve equivalence with that of their parent

radionuclide within a decay series. This equilibrium is crucial to guarantee that the activities of daughter nuclides precisely mirror the radioactivity of the original parent nuclide, thus securing accurate and reliable spectrometric readings (IAEA, 2014).

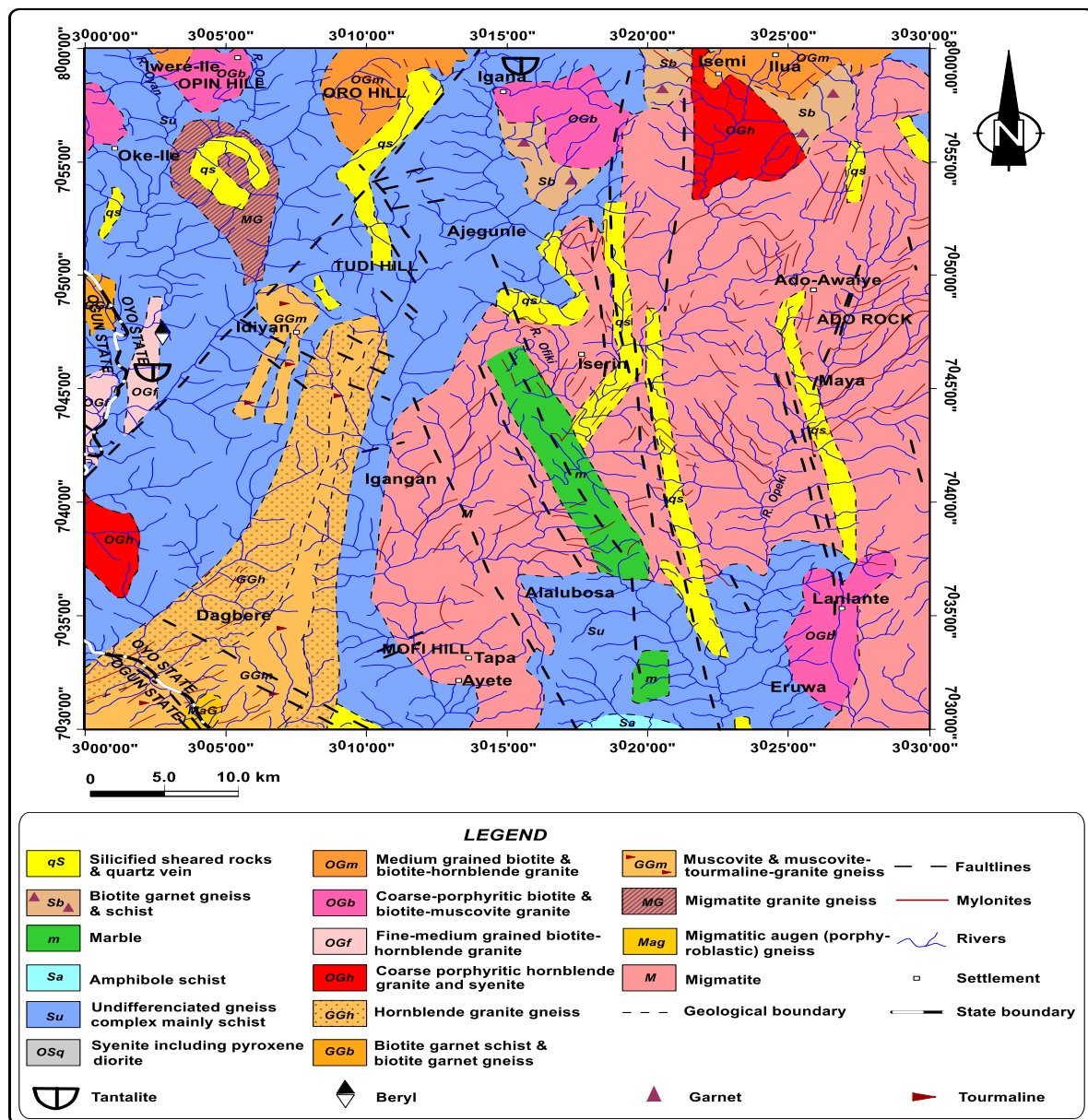


Figure 2: Geological Map of the Study Area

Measurement of Radionuclide Concentration

Calibration of the gamma-ray detection system was performed utilizing standard reference materials that contained certified radionuclide

concentrations, including well-recognized isotopic sources such as ^{137}Cs and ^{60}Co . This guaranteed the spectrometer's precision and measurement dependability. The soil samples were analyzed using a high-purity 2" \times 2"

thallium-activated sodium iodide NaI(Tl) vertical detector manufactured by Canberra, which was coupled to an ORTEC 456 amplifier. The detector was connected to the MAESTRO software, which facilitated real-time spectrum acquisition and enabled the comparison of recorded gamma-ray energies with a library of known isotopic emissions. The spectrometry setup achieved an energy resolution of 2.0 keV and a relative efficiency of 33% at a gamma energy of 1.33 MeV. Each sample was counted for 10,800 seconds to minimize statistical uncertainties and enhance measurement precision. Throughout the analytical process, both the measurement geometry and sample configuration were meticulously maintained in accordance with standard laboratory procedures. Calibration of the detector's energy and efficiency was carried out using reference standards supplied by the International Atomic Energy Agency (IAEA, 2003). The activity concentrations of radionuclides ^{226}Ra , ^{232}Th , and ^{40}K were quantified by analyzing gamma spectra using a dedicated computational program. The photopeaks selected for these determinations included the 1460 keV peak for ^{40}K , the 1764.5 keV line attributed to ^{214}Bi (a decay product of ^{238}U , serving as a proxy for ^{226}Ra), and the 2614.5 keV peak corresponding to ^{208}Tl in the ^{232}Th decay chain, with results expressed in becquerels per kilogram (Bq/kg). Background radiation levels were assessed using distilled water placed in containers identical in geometry to those used for soil samples. These background counts were then deducted from the gross counts to yield the net area beneath the chosen photopeaks,

$$A_C = \frac{cn}{P\gamma M\varepsilon} \quad (1)$$

In this context, cn represents the net count rate, obtained by deducting background radiation counts from the total detected counts specifically within the gamma photopeak of interest. The term $\varepsilon\gamma$ denotes the absolute detection efficiency of the system at the specific energy associated with the photopeak. Additionally, $P\gamma$ refers to the gamma emission probability for that energy level, while t indicates the total counting duration, and $M\varepsilon$ is

the mass of the prepared soil sample used for the analysis (Gilmore, 2011).

Estimation of Radiological Parameters

Evaluating potential radiological health effects is a critical aspect of environmental radiation monitoring, as it provides insight into both personal and ecological risks associated with ionizing radiation exposure. This study considered a suite of radiological indices to assess such hazards.

Absorbed Dose (D)

The absorbed dose rates in outdoor environments (D), resulting from gamma radiation in the air at a height of 1 metre above the ground, were determined for the uniform distribution of naturally occurring radionuclides ^{226}Ra , ^{232}Th , and ^{40}K in accordance with the guidelines established by UNSCEAR (2020). The absorbed dose rate (D) represents the amount of energy deposited by ionizing radiation per unit mass of material or biological tissue, expressed in grays (Gy) and reported in this study in nanograys per hour (nGy/h). It was computed based on the specific activity concentrations of the three naturally occurring radionuclides detected in the soil samples. Contributions from anthropogenic or minor radionuclides such as ^{137}Cs , ^{131}I , and ^{90}Sr were excluded because of their minimal effect on the total external dose rate. The absorbed dose rate (D) was evaluated using the following equation:

$$D(\text{nGy h}^{-1}) = 0.0414A_K + 0.461A_{Ra} + 0.623A_{Th} \quad (2)$$

Where A_K , A_{Ra} , and A_{Th} , are the activity concentrations ^{40}K , ^{226}Ra , and ^{232}Th respectively while 0.0414, 0.461, and 0.623 are the respective dose conversion factors recommended by UNSCEAR for each radionuclide

Annual Effective Dose (AED)

The annual effective dose serves as a key parameter for assessing potential health risks associated with exposure to environmental gamma radiation. It represents the biologically relevant fraction of the absorbed dose, accounting for stochastic effects such as cancer that may result from long-term, low-level exposure. To estimate the annual effective dose (AED) from the previously determined

absorbed dose rate (D), two conversion factors recommended by (UNSCEAR, 2000) were employed: a dose conversion coefficient of 0.7 Sv/Gy, which converts the absorbed dose in air to an equivalent effective dose in human tissue by considering radiation type and biological response, and occupancy factors of 0.42 for outdoor and 0.58 for indoor exposure. These occupancy values correspond to typical exposure patterns in mining environments, where workers are outdoors from 8:00 a.m. to 5:00 p.m. daily. Based on these parameters, the annual outdoor effective dose (OAED) and annual indoor effective dose (IAED), expressed in millisieverts per year (mSv/y), were determined using the following equations:

$$\text{OAED (mSv-1)} = D (\text{nGyh-1}) \times 8760(\text{hy-1}) \times 0.7(\text{SvGy-1}) \times 0.42 \times 10^{-6} \quad (3)$$

$$\text{IAED (mSv-1)} = D (\text{nGyh-1}) \times 8760(\text{hy-1}) \times 0.7(\text{SvGy-1}) \times 0.42 \times 10^{-6} \quad (4)$$

Where, D denotes the absorbed dose rate in nGy/h; 8760 represents the total number of hours in a year; 0.7 Sv/Gy is the dose conversion coefficient that translates the absorbed dose in air to an effective dose in human tissue; 0.42 and 0.58 are the occupancy factors for outdoor and indoor environments, respectively; and the factor 10^{-6} is used to convert the dose from nanograys to millisieverts.

Radium Equivalent Activity (Raeq): To represent the combined radiological impact of ^{226}Ra , ^{232}Th , and ^{40}K using a single parameter, the Radium Equivalent Activity (Raeq) is employed. This index provides an integrated measure of the gamma radiation hazard by assuming that 370 Bq/kg of ^{226}Ra , 259 Bq/kg of ^{232}Th , and 4810 Bq/kg of ^{40}K contribute equally to the external gamma dose rate. The Raeq value is determined using Equation (4), which facilitates a comparative assessment of the radiological risks associated with varying concentrations of these radionuclides.

Annual Gonadal Dose Equivalent (AGDE): This quantifies the yearly radiation dose received by the reproductive organs and other radiation-sensitive tissues, which is significant

because of its potential genetic and hereditary effects on exposed populations. This dosimetric parameter evaluates the radiological burden arising from naturally occurring radionuclides— ^{226}Ra , ^{232}Th , and ^{40}K —and is computed using Equation (5)

$$AGDE = 3.09 A_{Ra} + 4.18 A_{Th} + 0.314 A_k \quad (5)$$

The coefficients 3.09, 4.18, and 0.314 signify the dose conversion factors corresponding to the respective radionuclides' contributions to gonadal radiation exposure. This metric is critical in assessing the possible genetic impacts of radiation on exposed populations, particularly in environmental and public health risk evaluations.

Activity Utilization Index (AUI): Given the prevalent use of sand and soil-based materials as aggregates in construction within the study area, the Activity Utilization Index (AUI) was formulated to evaluate the gamma radiation exposure risk numerically for building materials containing natural radionuclide ^{226}Ra , ^{232}Th , and ^{40}K . The AUI serves as a composite index that accounts for the combined radiological impact of these radionuclides in structural materials. It facilitates a more accurate estimation of the external gamma dose rate potentially emitted into indoor or outdoor environments due to construction practices. The index was calculated using Equation (6), incorporating standardized weighting factors that reflect the relative radiological significance of each radionuclide. This assessment allows for the determination of whether the materials in use pose a radiological hazard that exceeds recommended safety thresholds.

$$\text{AUI} = \left(\frac{A_{Ra}}{50\text{Bq/kg}} \right) F_{Ra} + \left(\frac{A_{Th}}{50\text{Bq/kg}} \right) F_{Th} + \left(\frac{A_k}{500\text{Bq/kg}} \right) F_k \quad (6)$$

In the above equation, A_{Ra} , A_{Th} , and A_k represent the measured specific activities of ^{226}Ra , ^{232}Th , and ^{40}K , respectively, expressed in Bq/kg. The corresponding factors F_{Ra} , F_{Th} , and F_k , with values of 0.461, 0.623, and 0.0414, indicate the fractional contributions of ^{226}Ra , ^{232}Th , and ^{40}K to the total gamma dose rate. The recommended average activity limits for soils are 50 Bq/kg for ^{226}Ra , 50 Bq/kg for ^{232}Th , and 500 Bq/kg for ^{40}K . Ideally, the Activity

Utilization Index (AUI) should not exceed 1, as values greater than this threshold indicate an unacceptable level of radiation risk.

Representative Gamma Index ($I_{\gamma r}$): This serves as a benchmark for identifying building construction materials that might present a radiological risk to inhabitants (Jibiri and Okeyode, 2011). It acts as an indicator of the possible external gamma radiation hazard stemming from naturally occurring radionuclides (Ravisankar *et al.*, 2015). The value of $I_{\gamma r}$ was determined using the formula outlined in equation 7 (Jibiri *et al.*, 2014).

$$I_{\gamma r} = \frac{A_{Ra}}{150} + \frac{A_{Th}}{100} + \frac{A_K}{1500} \quad (7)$$

In this context, A_{Ra} , A_{Th} , and A_K refer to the specific activity concentrations of ^{226}Ra , ^{232}Th , and ^{40}K , respectively, expressed in Bq/kg. For the associated radiation hazard to be deemed negligible, the value of $I_{\gamma r}$ should remain below unity (≤ 1).

External and Internal Hazard Indices (H_{ex} and H_{in}):

They are quantitative indicators used to evaluate the potential radiological risks from external gamma radiation and internal exposure caused by radon gas and its short-lived decay products, respectively. The H_{ex} value was computed using Equation (8).

$$H_{ex} = \frac{A_{Ra}}{370} + \frac{A_{Th}}{259} + \frac{A_K}{4810} \quad (8)$$

Similarly, the internal risk posed by radon and its radioactive decay products is managed through the internal hazard index, H_{in} , which is determined using equation 9.

$$H_{in} = \frac{A_{Ra}}{185} + \frac{A_{Th}}{259} + \frac{A_K}{4810} \quad (9)$$

In the above equations (8 and 9), A_{Ra} , A_{Th} , and A_K represent the activity concentrations of ^{226}Ra , ^{232}Th , and ^{40}K , for the samples, in Bq kg^{-1} .

Excess Lifetime Cancer Risk (ELCR): It estimates the likelihood of individuals within a population developing cancer over a lifetime as a result of continuous exposure to ionizing radiation. It is calculated using Equation (10), which relates the ELCR to the previously determined average effective dose (AED).

$$ELCR = AEDE \times DL \times RF \quad (10)$$

Here, DL represents a life expectancy of 70 years, while RF denotes the risk factor, which is specified as 0.05 Sv^{-1} for stochastic effects.

Result and Discussion

Activity Concentration and Radium Equivalent in Soil Samples

Table 1 presents the activity concentrations of the naturally occurring radionuclides ^{40}K , ^{226}Ra , and ^{232}Th , along with their corresponding radium equivalent activity (Raeq), in soil samples collected from active mining areas, abandoned pits, and unmined (control) locations. In active mining sites, ^{40}K activity concentrations ranged from $136.5 \pm 35.19 \text{ Bq/kg}$ to $610.31 \pm 1.98 \text{ Bq/kg}$, with a mean value of $445.59 \pm 10.22 \text{ Bq/kg}$. The activity of ^{226}Ra was relatively low, varying from below detection limit (BDL) to $20.87 \pm 2.32 \text{ Bq/kg}$, averaging $3.07 \pm 1.58 \text{ Bq/kg}$. For ^{232}Th , concentrations ranged from BDL to $113.31 \pm 19.20 \text{ Bq/kg}$, with a mean of $43.34 \pm 3.22 \text{ Bq/kg}$. In abandoned mining areas, ^{40}K levels ranged between 259.31 ± 9.17 and $498.14 \pm 14.82 \text{ Bq/kg}$, with an average of $428.14 \pm 18.52 \text{ Bq/kg}$. The ^{226}Ra concentrations extended from BDL to $13.98 \pm 2.12 \text{ Bq/kg}$, yielding a mean of $7.40 \pm 1.32 \text{ Bq/kg}$, while ^{232}Th varied from BDL to $256.71 \pm 25.20 \text{ Bq/kg}$, averaging $80.16 \pm 12.22 \text{ Bq/kg}$. In the unmined (control) region, ^{40}K activity concentrations ranged from 147.14 ± 12.19 to $266.03 \pm 10.22 \text{ Bq/kg}$, with an average of $177.36 \pm 12.52 \text{ Bq/kg}$. The ^{226}Ra concentrations remained low, between BDL and $20.87 \pm 2.32 \text{ Bq/kg}$, averaging $3.07 \pm 1.58 \text{ Bq/kg}$, whereas ^{232}Th ranged from BDL to $71.43 \pm 2.74 \text{ Bq/kg}$, with a mean of $20.96 \pm 1.35 \text{ Bq/kg}$. When compared with the UNSCEAR (2000) global reference values of 400 Bq/kg for ^{40}K , 35 Bq/kg for ^{232}Th , and 30 Bq/kg for ^{226}R , the results reveal that both active and abandoned mining zones exceed the global averages for potassium and thorium, while the unmined area remains well below these levels. The low ^{226}Ra activity across all sites falls significantly under the global mean. The elevated ^{232}Th concentrations are likely attributable to the abundance of zircon-rich minerals in the study area. The radium equivalent activity (Raeq), which provides a

unified measure of the overall radiological impact from the three radionuclides, ranged from 20.48 to 393.34 Bq/kg, with an average value of 119.20 Bq/kg. This average remains below the recommended safety threshold of 370 Bq/kg, suggesting that the radiation levels pose no significant health risk. Nonetheless, spatial variations in Raeq across the sampling zones indicate localized differences likely influenced by geological and mineralogical factors in the soils.

Radiological Indices

Evaluation of Radiation Dose and

Associated Health Hazard Parameters

Table 2 presents the computed radiation dose and related health hazard parameters for the analyzed soil samples. The absorbed dose rates resulting from terrestrial gamma radiation range from 5.86 to 217.48 nGy/h, with an average value of 58.06 nGy/h. This mean slightly exceeds the global reference level of 55 nGy/h. For the Annual Effective Dose (AED), values derived from soils in active mining sites vary between 0.02 and 0.76 mSv/year, with a mean of 0.078 mSv/year. In comparison, samples from non-mined regions show a narrower range of 0.09 to 0.11 mSv/year and an average of 0.20 mSv/year, which remains significantly below the world average benchmark of 0.460 mSv/year. The Annual Gonadal Dose Equivalent (AGDE) values fall between 42.86 and 1173.87 μ Sv/year, averaging 385.82 μ Sv/year, which is above the recommended safety limit of 300 μ Sv/year. This elevated value suggests a potentially higher radiological burden on reproductive tissues in certain locations. The External Hazard Index (H_{ex}) ranges from 0.02 to 1.06 with an average of 0.32, while the Internal Hazard Index (H_{in}) varies from 0.02 to 1.07, with a mean of 0.33. Both indices have mean values below the critical threshold of 1, indicating that the overall exposure levels remain within internationally accepted safety limits and that normal human activities in these areas do not pose significant radiological hazards. The Excess Lifetime Cancer Risk (ELCR) values span 0.07 to 2.66×10^{-3} , with an average of 0.71×10^{-3} , remaining below the

upper limit of 1×10^{-3} recommended for public exposure. This result implies that the lifetime cancer risk for individuals in the area is within permissible bounds. The Gamma Index ($I_{\gamma r}$), used to assess the suitability of materials for construction from a radiological perspective, ranges from 0.09 to 3.29, with an average value of 0.96. Although a few samples marginally exceed unity, the mean value remains below the recommended limit of 1, confirming that the investigated materials are generally safe for construction use. Figures 1 to 9 illustrate the frequency distributions of radionuclide concentrations across the study sites. In active mining zones, the distribution of ^{40}K (Figure 1) is approximately normal, reflecting moderate potassium levels, while ^{226}Ra and ^{232}Th (Figures 2 and 3) display left-skewed patterns, indicative of lower concentrations. In abandoned mining areas, Figures 4–6 show that ^{40}K follows a right-skewed distribution, suggesting elevated potassium content, whereas ^{226}Ra and ^{232}Th maintain left-skewed trends, pointing to reduced activity levels. For unmined (control) regions, as depicted in Figures 7–9, all radionuclides (^{40}K , ^{226}Ra , and ^{232}Th) exhibit left-skewed distributions, confirming that radionuclide concentrations in these areas remain relatively low.

Gamma-ray spectrometric analysis showed that potassium (^{40}K) recorded an average activity concentration of 412.71 ± 12.53 Bq/kg, slightly exceeding the global average of 400 Bq/kg. The mean concentrations of radium (^{226}Ra) and thorium (^{232}Th) were 4.18 ± 1.91 Bq/kg and 58.20 ± 8.78 Bq/kg, respectively. While the radium concentration remains below the global reference level of 30 Bq/kg, the thorium concentration is noticeably higher than the world average of 35 Bq/kg.

Comparative assessment of radionuclide levels across active, abandoned, and unmined sites indicates that soils from both active and disused mining areas contain higher thorium and potassium activities than those in unexplored regions. The elevated concentrations are likely linked to the natural enrichment of zircon-bearing minerals commonly found within the geological formation of the study area.

Table 1: Activity Concentration of Naturally Occurring Radionuclides and Radium Equivalents

S/N	CODE	^{40}K (Bq/kg)	^{226}Ra (Bq/kg)	^{232}Th (Bq/kg)	Raeq (Bq/kg)
1	ABUISE1	540.69 \pm 12.12	BDL	113.37 \pm 19.24	203.75
2	ABUISE2	606.44 \pm 7.30	2.81 \pm 1.11	BDL	49.511
3	ABUISE3	347.14 \pm 14.98	20.87 \pm 2.32	112.39 \pm 8.47	192.92
4	ABUISE4	610.31 \pm 8.48	BDL	68.51 \pm 12.03	144.96
5	ABUISE5	599.67 \pm 6.57	BDL	121.17 \pm 10.45	219.44
6	ABUISE6	562.08 \pm 23.09	BDL	BDL	20.48
7	IWERE1	136.50 \pm 35.19	BDL	BDL	10.51
8	IWERE2	272.84 \pm 12.25	BDL	31.18 \pm 1.56	26.45
9	IWERE3	159.71 \pm 13.70	BDL	71.43 \pm 3.55	114.45
10	IWERE4	208.06 \pm 11.25	BDL	BDL	16.02
11	IWERE5	449.80 \pm 7.22	BDL	BDL	141.24
12	IWERE6	456.56 \pm 12.56	BDL	28.53 \pm 2.55	262.62
13	AKOYA1	498.14 \pm 14.83	15.87 \pm 2.04	56.81 \pm 12.48	135.47
14	AKOYA2	503.949 \pm 6.57	BDL	BDL	39.31
15	AKOYA3	259.31 \pm 9.01	6.27 \pm 1.22	256.71 \pm 25.20	393.34
16	AKOYA4	391.78 \pm 8.72	4.73 \pm 1.18	47.06 \pm 5.20	102.201
17	AKOYA5	457.53 \pm 7.62	3.58 \pm 1.92	17.80 \pm 3.14	64.27
18	AKOYA 6	457.53 \pm 7.62	13.95 \pm 2.20	105.56 \pm 10.22	200.15
19	AIYETE1	136.50 \pm 14.81	BDL	BDL	42.86
20	AIYETE2	159.72 \pm 11.08	BDL	71.43 \pm 2.34	348.73
21	AIYETE3	266.08 \pm 10.22	BDL	BDL	83.55
22	AIYETE4	147.14 \pm 12.20	10.28 \pm 3.42	12.39 \pm 2.34	129.76
	MEAN	177.36 \pm 12.71	2.57 \pm 1.22	20.96 \pm 1.35	151.22
	UNSCEAR	400.00	30.00	35.00	370.00

Table 2: Radiological Parameters Estimated

S/N	CODE	EHI	RGI	ELCR	D (nGyhr $^{-1}$)	AEDE (mSvyr $^{-1}$)	AGDE (mSvyr $^{-1}$)
1	ABUISE1	0.55	1.49	0.84	93.01	0.24	643.66
2	ABUISE2	0.13	0.42	0.24	26.40	0.07	199.11
3	ABUISE3	0.56	1.49	0.85	94.01	0.24	643.28
4	ABUISE4	0.39	1.09	0.61	67.95	0.17	478.01
5	ABUISE5	0.59	1.61	0.90	100.32	0.26	694.79
6	ABUISE6	0.26	0.74	0.42	46.55	0.12	332.65
7	IWERE1	0.07	0.22	0.13	13.93	0.04	105.66
8	IWERE2	0.18	0.49	0.28	30.72	0.08	216.01
9	IWERE3	0.14	0.41	0.23	25.68	0.07	185.35
10	IWERE4	0.04	0.14	0.08	8.61	0.02	65.33
11	IWERE5	0.09	0.30	0.17	18.62	0.05	141.24
12	IWERE 6	0.21	0.59	0.33	36.68	0.09	262.62
	MEAN	0.27	0.75	0.42	46.87	0.12	330.64
13	AKOYA1	0.37	1.01	0.57	63.33	0.16	442.92
14	AKOYA2	0.10	0.34	0.19	20.86	0.05	158.24
15	AKOYA3	1.06	2.78	1.56	173.56	0.45	1173.85
16	AKOYA4	0.28	0.76	0.43	47.72	0.12	334.35
17	AKOYA5	0.54	1.45	0.82	91.14	0.23	628.01
18	AKOYA 6	0.17	0.51	0.29	31.68	0.08	229.13
	MEAN	0.42	1.14	0.64	71.38	0.18	494.42

Evaluation of Naturally Occurring Radionuclides Concentration and

19	AYETE 3	0.03	0.09	0.05	5.65	0.01	42.86
20	AYETE4	0.31	0.82	0.46	51.11	0.13	348.73
21	AYETE1	0.06	0.18	0.10	11.02	0.03	83.55
22	AYETE2	0.11	0.29	0.17	18.55	0.05	129.76
	MEAN	0.12	0.34	0.19	21.58	0.06	151.22
	UNSCEAR	1.00	1	1.00	55.00	0.46	300.00

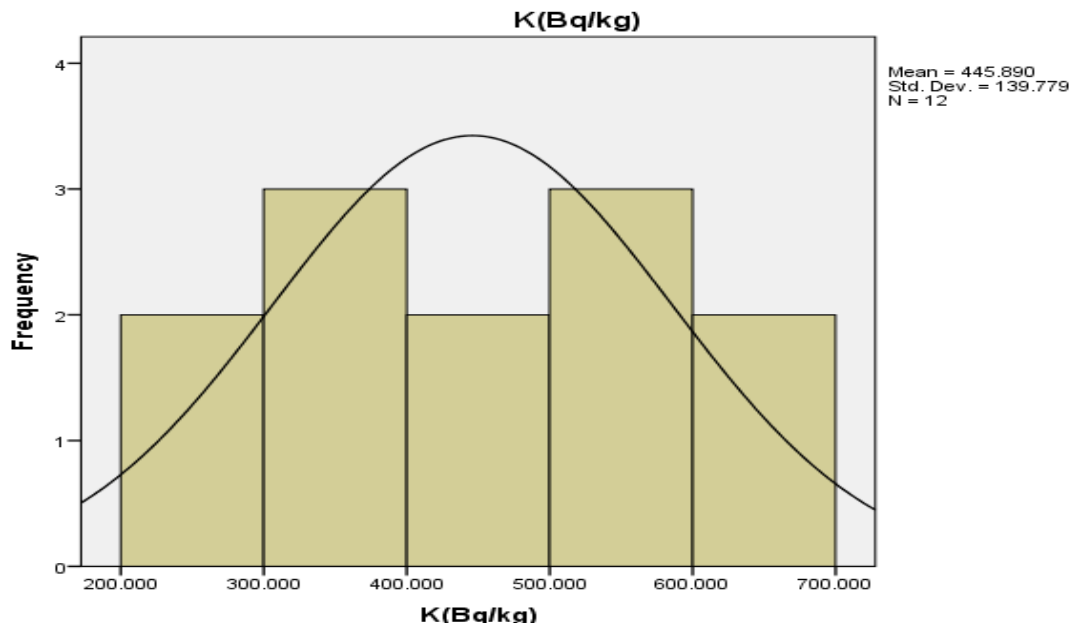


Figure 1: Distribution of Activity Concentration Frequency due to ^{40}K in Soil samples (Active mining site)

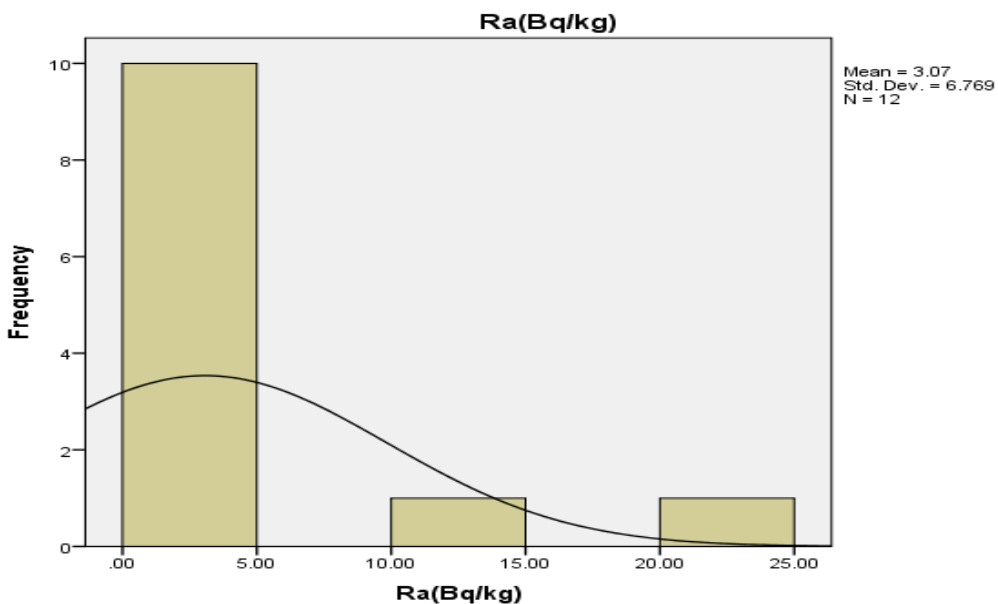


Figure 2: Distribution of Activity Concentration Frequency due to ^{226}Ra in Soil Samples (Active mining site)

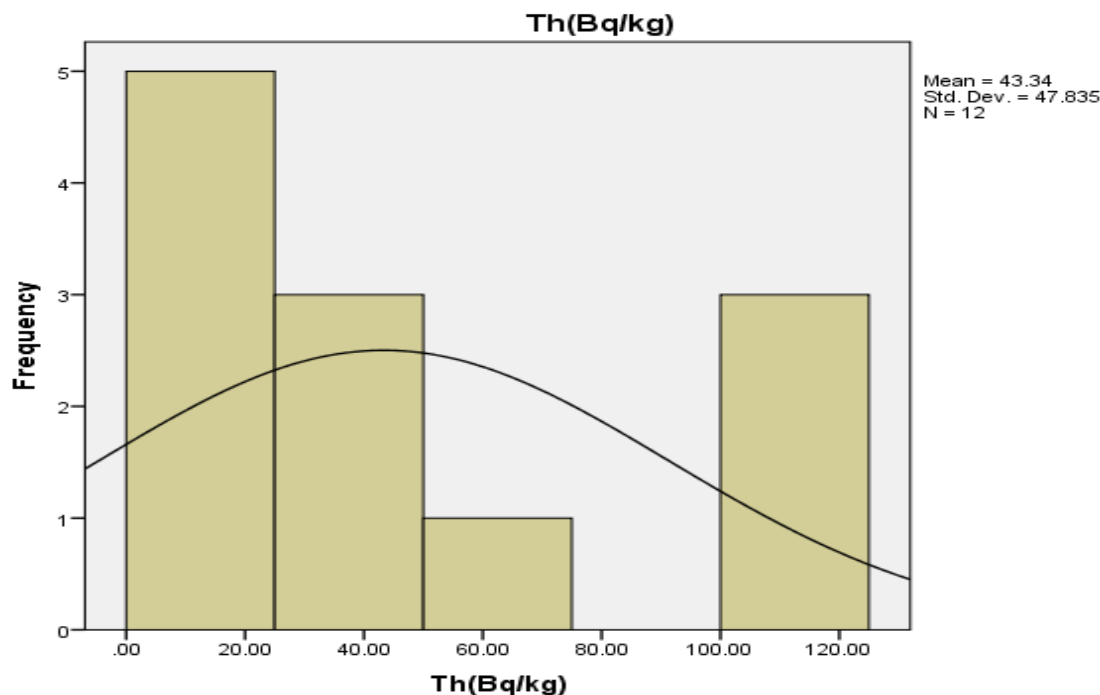


Figure 3: Distribution of Activity Concentration Frequency due to ^{232}Th in Soil Samples (Active mining site).

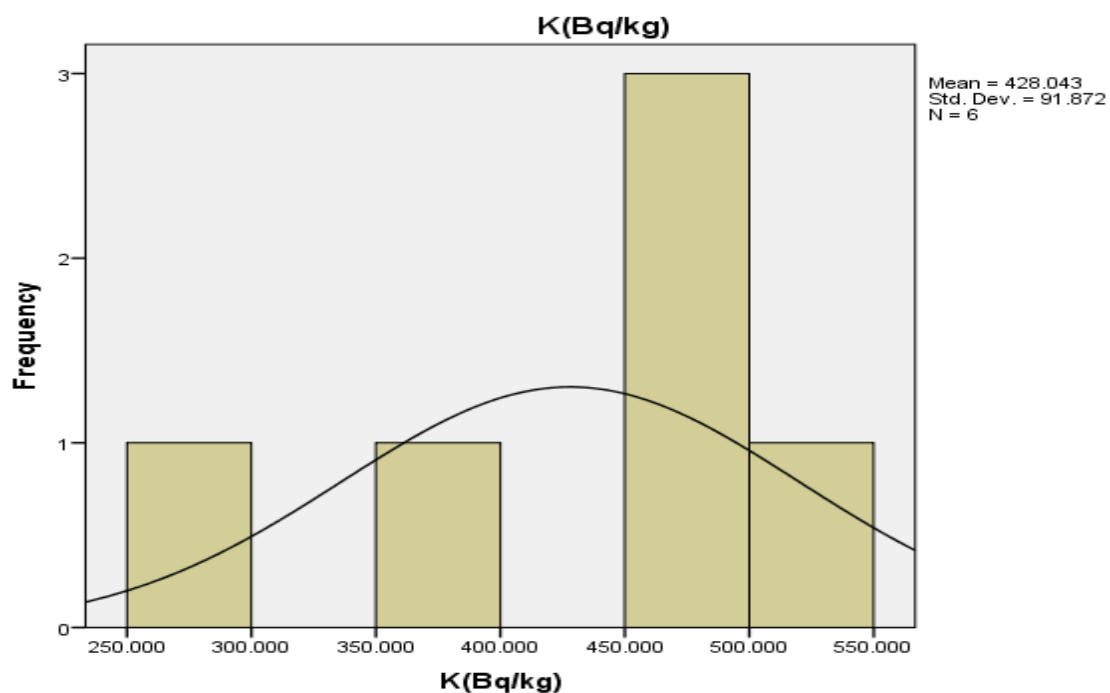


Figure 4: Distribution of Activity Concentration Frequency due to ^{40}K in Soil Samples (Abandoned mining site)

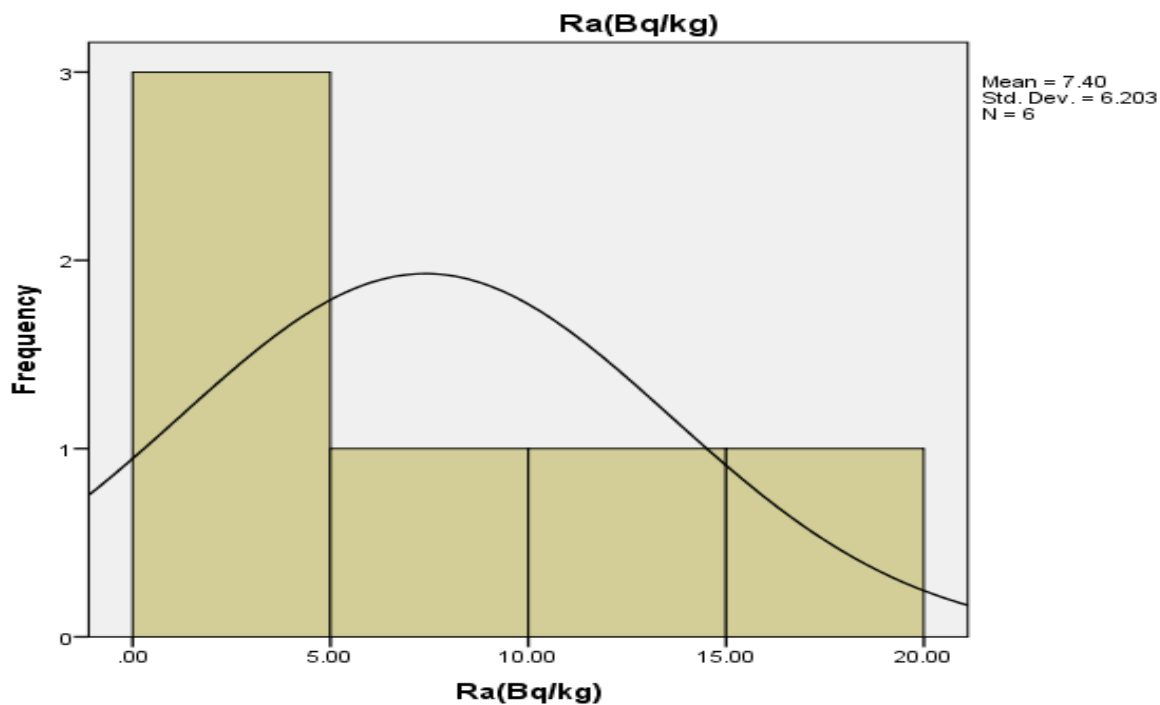


Figure 5: Distribution of Activity Concentration Frequency due to ^{226}Ra in soil samples (Abandoned mining site)

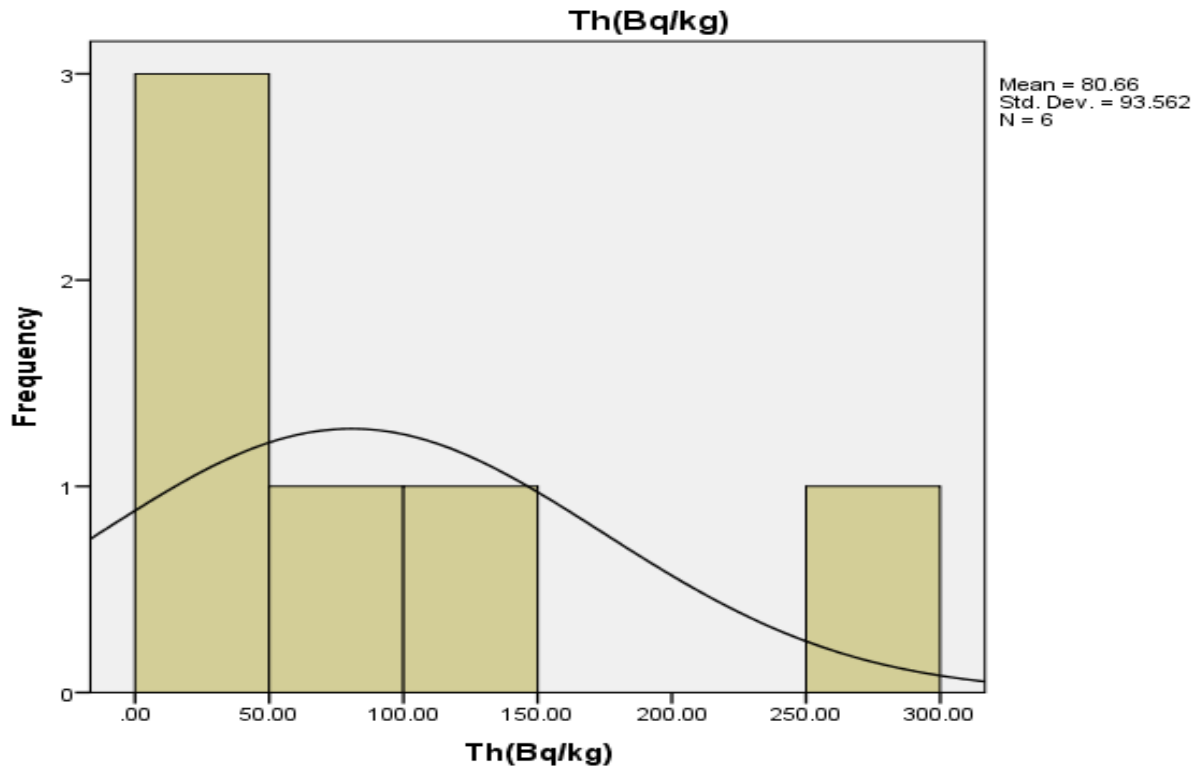


Figure 6: Distribution of Activity Concentration Frequency due to ^{232}Th in soil samples (Abandoned mining site).

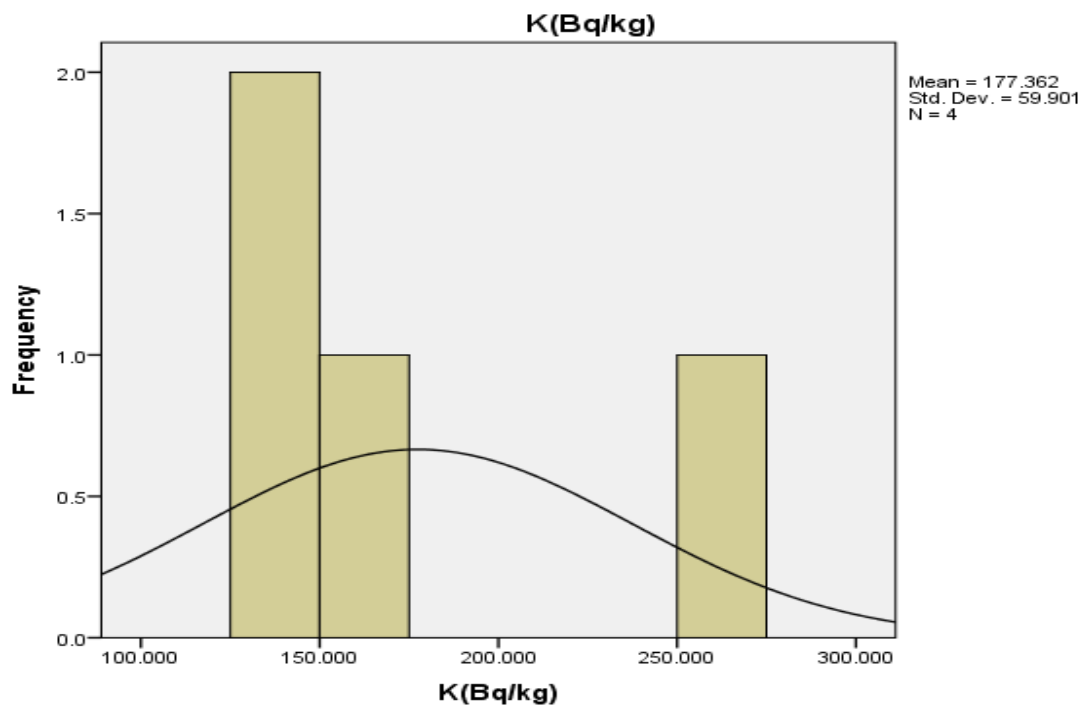


Figure 7: Frequency Distribution of Activity Concentration due to ^{40}K in Soil Samples (Unexplored site)

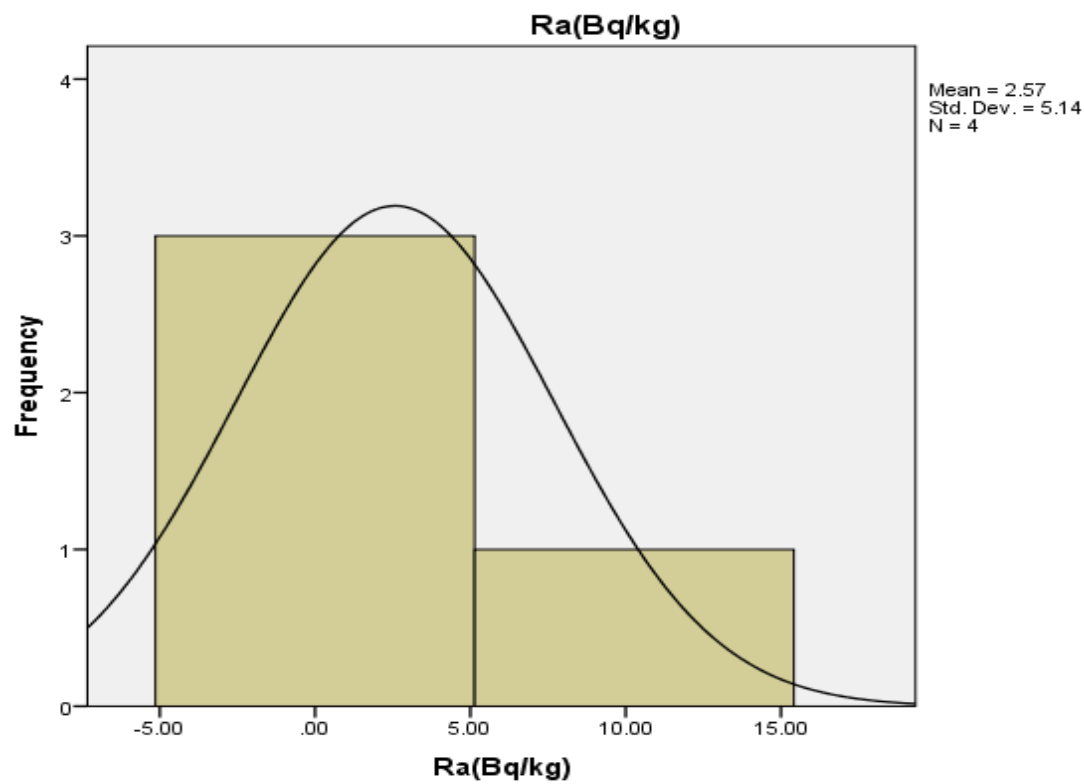


Figure 8: Distribution of Activity Concentration Frequency due to ^{226}Ra in Soil Samples (Unexplored site)

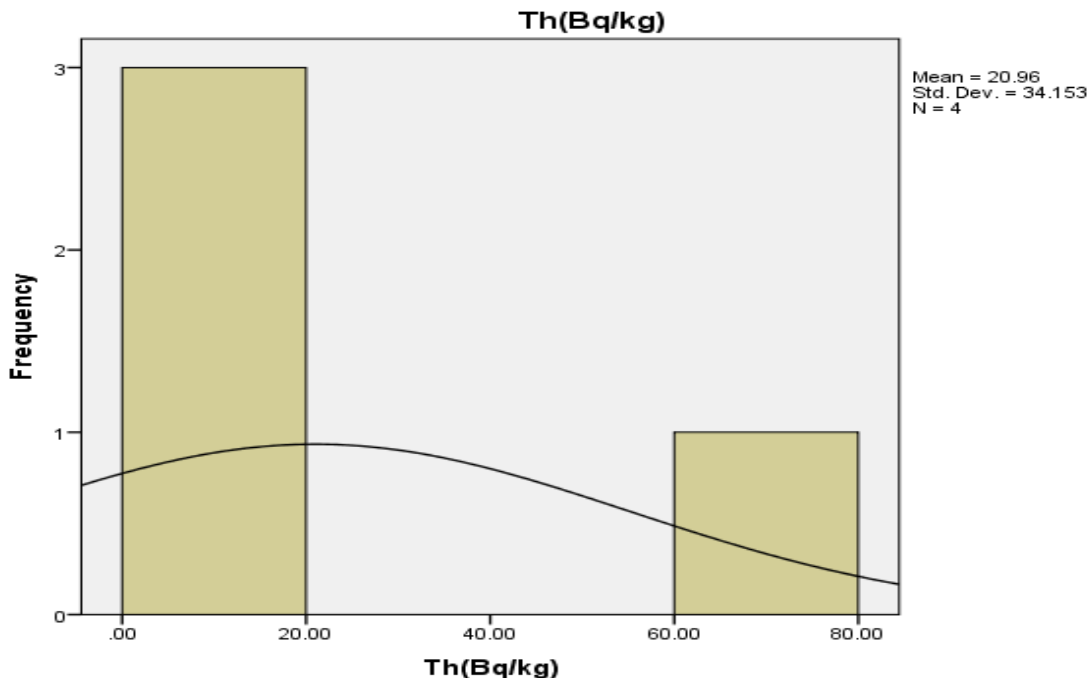


Figure 9: Distribution of Activity Concentration Frequency due to ^{232}Th in Soil Samples (Unexplored site).

Conclusion

This study has underscored the potential environmental and radiological health implications associated with small-scale mining activities, particularly within the Iwere-Ile region of Oyo State, Nigeria. Analysis of soil samples from both active and abandoned mining sites revealed elevated concentrations of naturally occurring radionuclides, especially ^{40}K and ^{232}Th , which exceeded global average values by approximately 15% and 9%, respectively. The measured terrestrial gamma radiation dose rates ranged from 5.86 to 217.48 nGy/h, with the mean value surpassing the global reference standard. Similarly, the annual gonadal dose equivalent (AGDE) values were found to exceed recommended safety thresholds, indicating potential long-term radiological health risks to individuals residing or working in proximity to the mining sites. However, both the external (H_{ex}) and internal (H_{in}) hazard indices remained below the critical limit of unity, suggesting that, under current conditions, the study areas are radiologically safe for general occupational and communal activities. The findings emphasize the

importance of continuous environmental surveillance and preventive interventions to minimize radiation exposure among local populations and workers. Moreover, the study advocates for the implementation of sustainable mining practices that balance economic development, public health protection, and environmental conservation. To effectively assess and manage the risks linked with small-scale mining, future research should focus on long-term monitoring and comprehensive radiological risk assessments. The integration of advanced analytical tools, such as high-resolution gamma-ray spectrometry combined with geospatial mapping technologies, will enhance the precision of environmental evaluations. Such data-driven and integrated approaches will enable policymakers and stakeholders to develop targeted mitigation strategies aimed at reducing environmental contamination, preserving ecological integrity, and protecting the health of communities dependent on mining for their livelihoods. Strategic, evidence-based interventions will be vital for establishing a safe and sustainable small-scale mining framework in the region.

References

Ajayi, I. R., and Ibikunle, S. B. (2013). Radiological assessment of environmental radioactivity in soil samples around a mining site in Osun State, Nigeria. *Radiation Protection Dosimetry*, 155(3): 351–357. <https://doi.org/10.1093/rpd/ncs313>

Ajibade, A.C. and Wright, J.B., 1989. *The Togo–Benin–Nigeria shield: Evidence of crustal evolution*. Precambrian Research, 44: 1–21.

Arogunjo, A. M., Ofuga, E. E., and Afolayan, O. (2004). Levels of natural radionuclides in soils at the International Institute of Tropical Agriculture (IITA), Ibadan, Nigeria. *Nigerian Journal of Physics*, 16: 25–29.

Beretka, J., and Mathew, P. J. (1985). Natural radioactivity of Australian building materials, industrial wastes and by-products. *Health Physics*, 48(1): 87–95 <https://doi.org/10.1097/00004032-198501000-00007>

International Atomic Energy Agency. (2003). *Radiation Protection against Radon in Workplaces Other than Mines* (IAEA Safety Reports Series No. 33). IAEA.

International Atomic Energy Agency. (2014). *Safety Reassessment for Research Reactors in the Light of the Accident at the Fukushima Daiichi Nuclear Power Plant* (IAEA Safety Reports Series No. 80). IAEA.

Jibiri N.N, Emelue H.U and Eke B.C. (2014) Excess lifetime cancer risk due to gamma radiation in and around Warri refining and petrochemical company in Niger Delta Nigeria. *BJMMR* 4(13): 2590–2598. doi: 10.9734/BJMMR/2014/7180

Jibiri, N. N. and Okeyode, I. C. (2011). Activity concentrations of natural radionuclides in the sediments of Ogun River, Southwestern Nigeria. *Radiation protection dosimetry*, 147(4): 555–564.

Jibiri, N. N. and Okeyode, I. C. (2012). Evaluation of radiological hazards in soils from Southwestern Nigeria. *Journal of Environmental Radioactivity*, 111: 58–64. <https://doi.org/10.1016/j.jenvrad.2012.03.001>

Kurnaz, A., Küçükömeroğlu, B., Keser, R., Okumusoglu, N. T., Korkmaz, F., Karahan, G., and Çevik, U. (2007). Determination of radioactivity levels and hazards of soil and sediment samples in Fatsa, Turkey. *Journal of Environmental Radioactivity*, 99(2): 284–290. <https://doi.org/10.1016/j.jenvrad.2007.06.001>

Obaje, N.G., (2009). *Geology and Mineral Resources of Nigeria*. Springer, Berlin.

Oyawoye, M.O. (1964). The geology of the Nigerian Basement Complex. *Journal of Mining and Geology*, 1(2): 87–102.

Rahaman, M.A. (1976). *Review of the Basement Geology of Southwestern Nigeria*. In: Kogbe, C.A. (Ed.), *Geology of Nigeria*. Elizabethan Publishing Co., Lagos, pp.41–58.

Rahaman, M.A. (1988). *Recent advances in the study of the Basement Complex of Nigeria*. In: Oluyide, P.O. et al. (Eds.), *Precambrian Geology of Nigeria*. Geological Survey of Nigeria, Kaduna, pp.11–43.

Ravisankar, R., Chandramohan, J., Chandrasekaran, A., Jebakumar, J. P. P., Vijayalakshmi, I., Vijayagopal, P., and Venkatraman, B. (2015). Assessments of radioactivity concentration of natural radionuclides and radiological hazard indices in sediment samples from the East coast of Tamilnadu, India with statistical approach. *Marine Pollution Bulletin*, 97(1-2): 419–430.

Tufail, M., Nasim-Akhtar, and Waqas, M. (2006). Measurement of terrestrial radiation hazards in soil samples from Pakistan *Radiation Protection Dosimetry*, 120(1–4): 399403. <https://doi.org/10.1093/rpd/nci595>

Turner, D.C., Oades, M.J. and Binks, R.M. (1983). *Proterozoic rocks of the Dahomeyan belt in Nigeria*. In: *Precambrian Geology of West Africa*. Elsevier, Amsterdam, pp.87–101.

UNSCEAR (2000). Sources and Effects of Ionizing Radiation. United Nations Scientific Committee on the Effects of Atomic Radiation Report to the General Assembly. United Nations, New York.

Evaluation of Naturally Occurring Radionuclides Concentration and

IAEA (2003). Radiation Protection and Safety of Radiation Sources: International Basic Safety Standards. IAEA Safety Series No. 115, Vienna.

UNSCEAR (2008). Sources and Effects of Ionizing Radiation. Report to the General Assembly with Scientific Annexes. United Nations, New York.

UNSCEAR, (2000). Dose assessment methodologies. Report to the General Assembly, Annex A, United Nation Scientific Committee on Atomic Radiation, ISBN 92-1-142228-7. 20–25.USA.